

[Invited] Principles and applications of real-time synthetic multi-exposure laser speckle contrast perfusion imaging

Martin Hultman^{1,2}, Marcus Larsson¹, Ingemar Fredriksson^{1,2}, Tomas Strömberg¹

¹ Department of Biomedical Engineering, Linköping University, Sweden

² Perimed AB, Järfälla-Stockholm, Sweden

E-mail: martin.o.hultman@liu.se

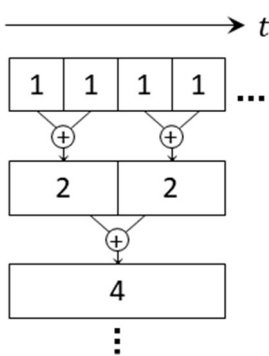
Abstract: Multi-exposure laser speckle contrast imaging (MELSCI) enables measurements of microcirculatory blood perfusion by analysis of speckle contrast as a function of exposure time. Recently, the technique has been made real-time by a combination of two main innovations. First, by hardware-accelerated calculation of synthetic exposure times, where multi-exposure is obtained by on-chip cumulative summation of high-speed sequences of speckle images. Second, by perfusion models based on machine learning. The combination allows continuous real-time imaging of perfusion at framerate and resolution sufficient to capture the spatiotemporal dynamics of the microcirculation. This opens new possibilities for analysis methods and clinical applications.

Keywords: Microcirculation, Blood perfusion, Multi-exposure laser speckle contrast imaging, Machine learning

1. Synthetic multi-exposure by cumulative sums

Multi-exposure laser speckle contrast imaging has in recent years shown great promise to enhance the interpretation and understanding of microcirculation blood perfusion measurements. Compared to traditional single-exposure laser speckle contrast imaging (LSCI), MELSCI captures more information about the speckle decorrelation and thus enables more informed models of perfusion. However, this has come at the expense of the simplicity of data acquisition in LSCI. Three different methods have been proposed for the acquisition of multi-exposure images – modulated illumination with constant exposure time [1], constant illumination with coded shutter acquisition [2], and synthetic multi-exposure by digital accumulation of high framerate image sequences [3]. Of these, only synthetic multi-exposure fully captures the speckle movements without loss of information due to inter-frame delays.

One method of efficiently computing synthetic exposure times is by binary tree summation of successive pairs of speckle images [4]. For example, using 64 speckle images acquired with 1 ms exposure time without interframe delay, each pair is summed to create 32 speckle images with double the exposure time, 2 ms. The successive pairs of these images are then summed again to create 16 images with 4 ms exposure time. This continues until all 64 original images have been accumulated into a single image with 64 ms exposure time. In total, this yields



images at exponentially increasing exposure times 1, 2, 4, 8, 16, 32, and 64 ms, efficiently covering a wide exposure range in $\mathcal{O}(N)$ accumulations. A smaller example of this is illustrated in Figure 1.

Figure 1: Example illustration of binary tree accumulation for efficient calculation of synthetic exposure times.

2. Inherent noise reduction in synthetic multi-exposure

The main advantage of synthetic multi-exposure method over other acquisition schemes is that the full acquisition range (64 ms in this example) can be considered for all exposure times. For example, the 64 images with 1 ms exposure time cover the same acquisition range as the 32 images with 2 ms exposure time, which covers the same as the 16 images with 4 ms exposure time, etc. This allows an inherent noise reduction in the speckle contrast images, by computing the 64 contrast images at 1 ms exposure time and taking an average. In general, for exposure time T there are $64/T$ independent speckle images which can be analyzed and averaged. Dark noise (thermal) and shot noise in the speckle images give rise to unwanted variance which reduces the contrast-to-noise ratio of the speckle contrast images [5]. The noise variance can be summarized as

$$\sigma_{\text{noise}}^2 = N_{\text{shot}}\langle I \rangle + N_{\text{dark}}$$

where N_{shot} and N_{dark} are constants that must be measured experimentally. The relative contribution of shot noise to measured speckle contrast decreases linearly with increasing intensity, thus correspondingly with accumulated exposure time as well. As such, the noise is higher for lower exposure times, but this is exactly canceled out by the averaging over independent contrast images [6]. The same applies for dark noise, resulting in an inherent ability of synthetic multi-exposure to retain the same noise characteristics across exposure times without the need for modulation of either the light source or the acquisition schedule. Furthermore, the averaging operation incorporates the speckle information from the full 64 ms into each exposure time, resulting in no loss of information, and allows the use of a multi-exposure noise model common across all exposure times:

$$\sigma_{\text{noise}}^2(T) = TN_{\text{shot}}\langle I \rangle + TN_{\text{dark}} + T^2N_{\text{const}}$$

where the new noise constant N_{const} accounts for static spatial inhomogeneities between pixels, for example due to poor calibration [6].

3. Implementation in highly parallel computation hardware

The main drawback of synthetic multi-exposure is the immense data volumes generated by the high-speed acquisition. A continuous stream of 1-megapixel, 12-bit monochrome images at 1000 frames-per-second yields a throughput of 1.5 GB/s, which requires specialized hardware to perform the processing in real-time. This has been demonstrated using a field-programmable gate array (FPGA) closely integrated with the high-speed CMOS sensor [4, 7]. The accumulation of synthetic exposure times and the calculation of speckle contrasts were performed in a highly parallel implementation directly in the FPGA before transferring the computed multi-exposure contrast to a connected computer. This is so far the only presented solution for real-time continuous acquisition and processing of synthetic MELSCI [4, 6].

4. Perfusion models based on machine learning

After acquiring and processing the multi-exposure contrast images, a model for estimating the corresponding perfusion is required. Conventional single-exposure LSCI is fast since it uses a direct model where the perfusion is assumed to be inversely proportional to the speckle contrast [8, 9], for example

$$P_{SE} = \frac{1}{K^n} - 1$$

where n is either 1 or 2. Models relating perfusion to multi-exposure contrast are, by comparison, much more complex [1]. Directly applying these models thus requires non-linear fitting to measured data, which is a prohibitively slow process for real-time perfusion imaging. To address this issue, a methodology based on machine learning has been proposed, in which a neural network is trained to estimate the perfusion directly from the multi-exposure contrast. This offloads the time-consuming computations to the network training and has been demonstrated to increase the processing speed by a factor of more than 1000 compared to methods requiring non-linear fitting [10]. This

enables real-time application of perfusion imaging with framerates sufficiently high (e.g., 15.6 fps using 64 contrast images at 1 ms exposure time) to capture the dynamics of the microcirculation blood flow [6]. An example is presented in Figure 3.

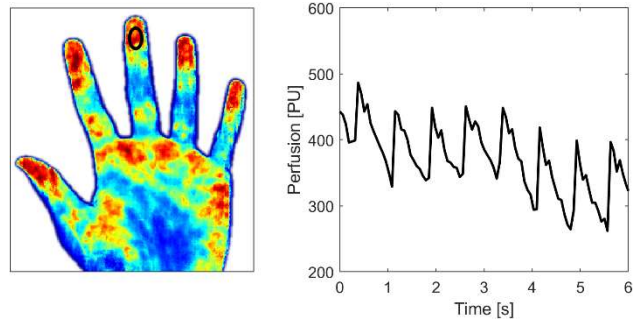


Figure 3: ANN-based perfusion computed from MELSCI data. Time-resolved curve is average perfusion in the black ellipse on the fingertip of the middle finger.

5. Clinical potential of perfusion imaging with high spatiotemporal resolution

The combination of continuous real-time imaging at high framerates and accurate perfusion models based on the information in the multiple exposure times, has high potential to increase the ease of interpretation and usefulness of the technique in clinical settings. It has been demonstrated how this can enable real-time perioperative monitoring of microvascular status during endovascular interventions of chronic limb-threatening ischemia (CLTI). It was shown that this technique can be used to detect the successful restoration of blood flow to the ischemic foot, but also to detect potential adverse events that would be undetectable using current macrovascular monitoring techniques, such as x-ray angiography [11]. These discoveries relied on the high framerate of perfusion images, enabling the detection of heart-related pulsations in the microcirculation, as well as the simultaneously high spatial resolution, enabling the detection of local occlusion in single toes. Figure 2 shows perfusion measured in the foot before and after surgery for CLTI, and demonstrates the high spatiotemporal resolution.

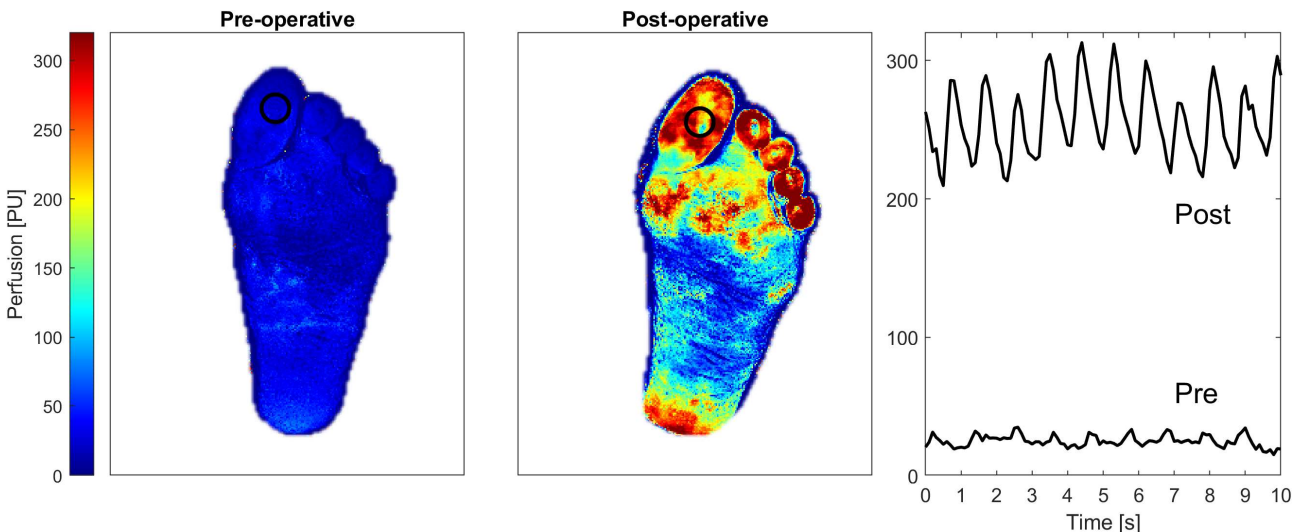


Figure 2: Perfusion measured pre- and post-operatively in a patient treated by endovascular surgery for chronic limb-threatening ischemia. Pulsatile flow is restored to the foot after surgery, indicating a successful intervention.

6. Advanced processing of MELSCI for improved physiological interpretations

A promising future prospect of MELSCI in combination with advanced perfusion models is the ability to extract new physiological information from the speckle data. One method to do so is to compute speed-resolved perfusion, where the perfusion signal is decomposed into physiologically relevant speed regions, as shown in Figure 4. This has been possible in single-point measurements using laser Doppler flowmetry [12, 13], but has only recently become possible in imaging with the new advancements in MELSCI-based systems [14]. Speed-resolved perfusion allows increased physiological insights by separating flow in arterioles and venules from flow in capillaries, since the smaller vessels in general correspond to slower blood flow. This allows further analysis of the nutritive capillary flow rather than the combination of large and small vessels, potentially opening the possibility of new clinical applications. In LDF, speed-resolved perfusion has been used to investigate the impairment of nutritive capillary flow in patients with diabetes [15].

The combination of high spatiotemporal resolution and continuous acquisition also enables new analysis methods of microvascular flowmotion, which have previously been limited to single-point measurements. By flowmotion analysis it is possible to obtain physiological information about the regulatory mechanisms in the vasculature, by analyzing the periodic oscillations in the perfusion signal at different time-scales [16-18]. Specifically, it was recently demonstrated how to apply wavelet frequency transforms to the MELSCI perfusion video sequences to extract physiological information about the regulatory mechanisms in the skin [19]. For single-point techniques, this analysis has shown promise as a marker for numerous pathologies, such as diabetes [20, 21], but the practical use has been limited due to the high heterogeneity in the microvasculature. This limitation was overcome using MELSCI and has high potential to increase the clinical applicability of flowmotion.

7. Conclusion

In conclusion, single-exposure LSCI has long been limited by the difficulty to interpret the data, as well as the inability to distinguish perfusion from tissues that are physiologically very different. MELSCI was proposed as a possible solution but has instead been held back by the increased technical requirements, limiting the technique to post-processing applications. With recent advances this has been solved, and real-time clinical applications are possible, while also gaining the benefits from the more informed perfusion models enabled by MELSCI. These advancements have high potential to lead to new and improved clinical applications based on an increased understanding of the microcirculation blood flow.

References

1. Parthasarathy, A.B., et al., *Robust flow measurement with multi-exposure speckle imaging*. Optics Express, 2008. **16**(3): p. 1975-1989.
2. Kagawa, K., [Invite Paper] *Functional Imaging with Multi-tap CMOS Pixels*. ITE Transactions on Media Technology and Applications, 2021. **9**(2): p. 114-121.
3. Dragojević, T., et al., *High-speed multi-exposure laser speckle contrast imaging with a single-photon counting camera*. Biomedical Optics Express, 2015. **6**(8): p. 2865-2876.
4. Hultman, M., et al., *A 15.6 frames per second 1-megapixel multiple exposure laser speckle contrast imaging setup*. Journal of Biophotonics, 2017. **11**(2).
5. Valdes, C.P., et al., *Speckle contrast optical spectroscopy, a non-invasive, diffuse optical method for measuring microvascular blood flow in tissue*. Biomedical Optics Express, 2014. **5**(8): p. 2769-2784.

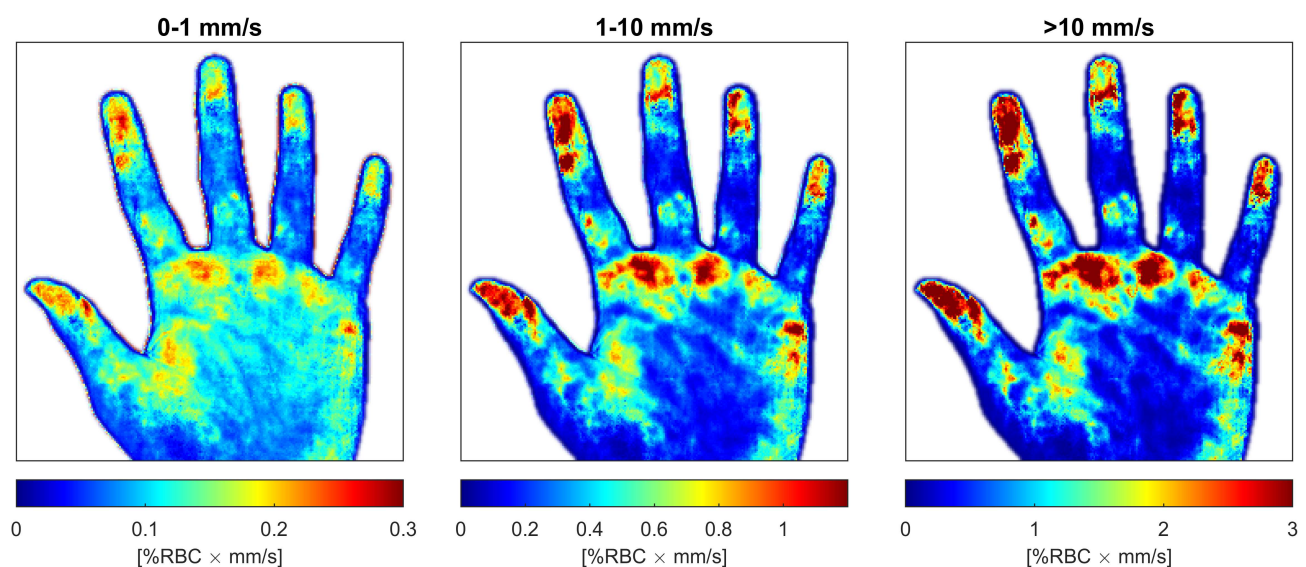


Figure 4: Speed-resolved perfusion, separating the perfusion signal into three distinct and physiologically relevant speed intervals, thus increasing the physiological interpretation of the data. Notice how the high-speed component is more concentrated to spots with high perfusion, indicating larger vessels where flow is generally higher. The low-speed component is more homogeneous, indicating flow related to smaller vessels and capillaries.

6. Hultman, M., et al., *Real-time video-rate perfusion imaging using multi-exposure laser speckle contrast imaging and machine learning*. Journal of Biomedical Optics, 2020. **25**(11): p. 1-15.
7. Sun, S., et al., *Multi-exposure laser speckle contrast imaging using a high frame rate CMOS sensor with a field programmable gate array*. Optics Letters, 2015. **40**(20): p. 4587-4590.
8. Briers, D., et al., *Laser speckle contrast imaging: Theoretical and practical limitations*. Journal of Biomedical Optics, 2013. **18**(6).
9. Liu, C., et al., *Choosing a model for laser speckle contrast imaging*. Biomedical Optics Express, 2021. **12**(6): p. 3571-3583.
10. Fredriksson, I., et al., *Machine learning in multiexposure laser speckle contrast imaging can replace conventional laser Doppler flowmetry*. Journal of Biomedical Optics, 2019. **24**(1).
11. Hultman, M., et al., *Comprehensive imaging of microcirculatory changes in the foot during endovascular intervention – A technical feasibility study*. Microvascular Research, 2022. **141**: p. 104317.
12. Fredriksson, I., et al., *Inverse Monte Carlo in a multilayered tissue model: merging diffuse reflectance spectroscopy and laser Doppler flowmetry*. Journal of Biomedical Optics, 2013. **18**(12): p. 1-15.
13. Fredriksson, I., M. Larsson, and T. Strömberg, *Model-based quantitative laser Doppler flowmetry in skin*. Journal of Biomedical Optics, 2010. **15**(5): p. 057002.
14. Hultman, M., et al., *Speed-resolved perfusion imaging using multi-exposure laser speckle contrast imaging and machine learning*. Submitted, 2022.
15. Fredriksson, I., et al., *Reduced arteriovenous shunting capacity after local heating and redistribution of baseline skin blood flow in type 2 diabetes assessed with velocity-resolved quantitative laser Doppler flowmetry*. Diabetes, 2010. **59**(7): p. 1578-84.
16. Bračič, M. and A. Stefanovska, *Wavelet-based analysis of human blood-flow dynamics*. Bulletin of Mathematical Biology, 1998. **60**(5): p. 919-935.
17. Fredriksson, I., et al., *Vasomotion analysis of speed resolved perfusion, oxygen saturation, red blood cell tissue fraction, and vessel diameter: Novel microvascular perspectives*. Skin Research and Technology, 2022. **28**(1): p. 142-152.
18. Kvandal, P., et al., *Low-frequency oscillations of the laser Doppler perfusion signal in human skin*. Microvascular Research, 2006. **72**(3): p. 120-127.
19. Hultman, M., et al., *Flowmotion imaging analysis of spatiotemporal variations in skin microcirculatory perfusion*. Microvascular Research, 2022: p. 104456.
20. Reynès, C., et al., *Concomitant Peripheral Neuropathy and Type 2 Diabetes Impairs Postexercise Cutaneous Perfusion and Flowmotion*. The Journal of Clinical Endocrinology & Metabolism, 2021. **106**(10): p. e3979-e3989.
21. Los-Stegienta, A., et al., *Differentiation of Diabetic Foot Ulcers Based on Stimulation of Myogenic Oscillations by Transient Ischemia*. Vasc Health Risk Manag, 2021. **17**: p. 145-152.